Published in final edited form as:
Nat Neurosci. 2005 March ; 8(3): 372–379.

Receptive field structure varies with layer in the primary visual cortex

Luis M Martinez[1], **Qingbo Wang**[2], **R Clay Reid**[3], **Cinthi Pillai**[2], **José-Mañuel Alonso**[4], **Friedrich T Sommer**[5], and **Judith A Hirsch**[2]

1*Department of Medicine, Campus de Oza, Universidad A Coruña, 15006, Spain.*

2*Department of Biological Sciences, University of Southern California, 3641 Watt Way, Los Angeles, California 90089-2520, USA.*

3*Department of Neurobiology, Harvard Medical School, 220 Longwood Ave., Boston, Massachusetts 02115, USA.*

4*Department of Biological Sciences, State University of New York College of Optometry, 33 West 42nd St., New York, New York 10036, USA.*

5*Redwood Neuroscience Institute, 1010 El Camino Real, Menlo Park, California 94025, USA.*

Abstract

Here we ask whether visual response pattern varies with position in the cortical microcircuit by comparing the structure of receptive fields recorded from the different layers of the cat's primary visual cortex. We used whole-cell recording *in vivo* to show the spatial distribution of visually evoked excitatory and inhibitory inputs and to stain individual neurons. We quantified the distribution of 'On' and 'Off' responses and the presence of spatially opponent excitation and inhibition within the receptive field. The thalamorecipient layers (4 and upper 6) were dominated by simple cells, as defined by two criteria: they had separated On and Off subregions, and they had push-pull responses (in a given subregion, stimuli of the opposite contrast evoked responses of the opposite sign). Other types of response profile correlated with laminar location as well. Thus, connections unique to each visual cortical layer are likely to serve distinct functions.

How does connectivity in striate cortex correlate with receptive field structure and, ultimately, with neural selectivity for elements of the visual scene? Anatomical studies show that each of the six cortical layers has a unique pattern of inputs and outputs[1-4]. Thus, it is possible to investigate the function of specific components of the cortical microcircuit by comparing neural response patterns at different laminar positions[5-20]. We took this approach to ask whether there are response properties exclusive to the first stage of cortical integration, where new response properties such as orientation sensitivity emerge[12].

Early studies suggested that orientation selectivity depends on the structure of the simple receptive field, an arrangement of elongated On and Off subregions with an antagonistic effect on one another[12,21-23]. This idea came from observations of responses evoked by stimuli placed at different positions in visual space. For instance, a bright contour aligned lengthwise with an On subregion produced strong excitation that diminished when the stimulus was rotated towards the orthogonal angle or was moved sideways to cover larger portions of an adjacent Off subregion[12]. The geometry of the simple cell's response was thought to result from an orderly pattern of convergence from On and Off thalamic relay cells[12,23-26].

Correspondence to: Judith A Hirsch.
Correspondence should be addressed to J.A.H. (jhirsch@usc.edu).

Later studies suggested that the two main physiological types of cell in the visual cortex, simple and complex, were generated at all levels of cortical processing and represented two ends of a continuous spectrum[27–32] (M.S. Jacob *et al*., *Soc. Neurosci. Abstr*. 910.13, 2003). An argument made to advance this view is that values for some parameters used to distinguish simple from complex cells are distributed unimodally rather than bimodally[29,32]. Yet, if the distribution of values for a given set of parameters is unimodal, but all cases that fall to one side of a cutoff are restricted to a particular layer, it could nonetheless be possible to correlate type of visual response with location in the cortical circuit.

Thus, to measure quantitatively the receptive fields of neurons at established laminar positions, we combined intracellular staining, whole-cell recording and a spatial mapping protocol. Over time, we were able to obtain information about anatomically identified cells in each cortical layer. We used two main measures to describe receptive field structure. First, we used an overlap index to assess the spatial segregation of On and Off subregions[33]. Second, we used a push-pull index to determine the presence and relative weight of antagonistic responses to stimuli of the opposite contrast within individual subfields[21–23,34–38]. Our finding is that cells with simple receptive fields, as judged by scores for both indices, are found exclusively in thalamorecipient zones, where they are the majority. Complex cells are found throughout the cortical depth, though their response characteristics change with laminar location. All told, we show that the simple receptive field is a unique feature of regions that receive thalamic input. More generally, our results support the view that each stage of the cortical microcircuit is designed to analyze different aspects of the visual stimulus.

RESULTS

To explore how cortical receptive fields vary with position in the cortical microcircuit, we mapped the spatial distribution of excitation and inhibition in the receptive fields of neurons at identified anatomical sites. We also studied thalamic relay cells, which supply visual cortex. Our sample, 88 cells in 58 adult cats, included neurons in the thalamus (n = 25), layer 4 and its borders (n = 34), layers 2+3 (n = 12), layer 5 (n = 6) and layer 6 (n = 11).

Synaptic structures of receptive fields

An overview of the receptive fields we recorded is provided by **Figures 1** and **2**. Each figure is organized according to station in the microcircuit, from the thalamus, to layer 4, to the superficial layers (layer 2+3) to the deep layers (layers 5 and 6). The stimulus was sparse noise (individually flashed bright and dark squares). The receptive fields are shown as grids in which each coordinate is represented by a pair of traces that show the averaged response to bright and dark stimuli. The dashed blue and red contours outline the general shape of the Off and On subregions, respectively.

The receptive field of an Off-center thalamic relay cell is shown in **Figure 1a**. Within each subregion, center and surround, stimuli of the reverse contrast evoked responses of the opposite sign: a push-pull pattern[21–23,35–37]. Dark squares at the center coordinates evoked an initial depolarization followed by a hyperpolarization that corresponded to withdrawal of the stimulus. Bright squares flashed at the same positions evoked the opposite response: a hyperpolarization succeeded by a depolarization. The responses from the surround, though weak (small spots are suboptimal stimuli for the surround), showed a push-pull pattern as well.

The majority of receptive fields (26 of 38) in thalamorecipient zones, layer 4 and its borders, and upper layer 6, were built of adjacent On and Off subregions; each subregion had a push-pull pattern, as in the thalamus. In cortex, however, the subregions lay side by side. This qualitative arrangement resembles simple receptive fields as first described[12] (**Figs. 1b-d**). A receptive field of a cell in layer 4 (**Fig. 1b**) had a strong Off subregion flanked by a smaller On

subregion. Throughout the Off subregion, dark squares evoked a strong initial depolarization whereas bright squares flashed in the same positions produced a hyperpolarization. A complementary pattern was seen in the On subregion. Push-pull was present for cells with different numbers of subregions or anatomical profiles. For example, push-pull was seen in all three subregions of the receptive field of a spiny stellate cell (**Fig. 1d**) and throughout the receptive field of a basket cell (**Fig. 1c**; see refs. [35,36]).

Most remaining cells (n = 37) lacked adjoining On and Off subregions, a spatial profile often termed complex[9,12,34]. Such cells responded in one of three main ways to the sparse-noise stimulus (**Fig. 2**). One pattern, typical of thalamorecipient zones, is shown for a spiny stellate neuron (**Fig. 2a**) and for a smooth cell (**Fig. 2c**). For both neurons, bright and dark squares produced excitatory responses throughout the field: a push-push rather than a push-pull profile. As for all cells at the first stage of cortical processing, the time course of the response followed the temporal envelope of thalamic activity[11]. A second group of cells, in layers 2+3, 5 or 6, responded only to one polarity of the stimulus: a push-null profile (**Fig. 2b,d**). The responses of these cells are brief and irregular, as is typical of cells that do not receive contact from the thalamus[11]. Last, many cells failed to respond to the sparse noise, though they responded vigorously to moving stimuli[11]. Such cells occupied later cortical stages: the upper tier of layers 2+3, layer 5 or the bottom half of layer 6. Thus, the response profile of complex cells at the thalamocortical level distinguishes them from complex cells in regions that do not receive direct afferent input.

The synaptic structure of the receptive field predicted the suprathreshold pattern of response. For simple cells (**Fig. 3a**), contour plots of the receptive field are shown in a single plot. For complex cells (**Fig. 3b**), maps of bright and dark responses are shown separately, in adjacent plots, so that On and Off responses can be compared. The receptive fields made with spikes were often smaller than those made with synaptic potentials, but the overall shape was similar. In rare instances, however, weak subregions remained subthreshold.

Spatial distribution of On and Off responses

We used an overlap index[33] to measure the spatial segregation of subregions within the receptive field (**Figs. 3c,d**). Values $\lesssim 0$ indicate separated subregions and those ≈ 1 denote symmetrically overlapped subregions (**Fig. 3c,** legend). The index did not resolve potential overlap between the outermost regions of each subfield (see Methods), and only cells that responded to dark and bright spots could be included. The cells qualitatively described as simple cells had values between −0.40 and 0.09 (−0.09 ± 0.12, mean ± s.d.; n = 26) and cells with scores from 0.32 to 0.84 (0.67 ± 0.16; n = 15) corresponded to a subset of those described qualitatively as complex.

We next compared the overlap indices from synaptic responses to those measured from spikes (**Fig. 3d**). (We were able to use only a subset of the population; for some cells, action potentials were blocked with QX-314, and in rare cases, subregions remained below spike threshold.) The distributions of the values for subthreshold (**Fig. 3d**, top) and suprathreshold (**Fig. 3d**, right) responses were similar (correlation coefficient r = 0.90; $P < 0.0001$). Still, most points in the scatter plot (**Fig. 3d**, center) that compares the two values for each cell fell below the line of unit slope; it is likely that the reduced width of the spike subfields emphasized even small disparities between the peaks of largely cospatial On and Off subfields and widened the distance between segregated On and Off subregions.

We further analyzed receptive field structure to include inhibition, using a push-pull index (measurements were restricted to the center of each subfield; see Methods). If stimuli of the opposite contrast evoked comparable amounts of push and pull, the index value was ≈0; a value ≈1 indicated push-null (numbers are absolute values) and a score ≈2 denoted push-push (**Fig.**

4a, bottom). Cells with separated On and Off subregions (**Fig. 3a**) had index values <<1 (histogram, **Fig. 4a**; range, 0.00–0.57; mean, 0.22 ± 0.17; *n* = 26). Conversely, almost all cells that lacked segregated On and Off subregions had values ≈1 (range, 0.91–1.10; mean, 0.97 ± 0.07; *n* = 8) or values approaching 2 (range 1.27–1.93; mean, 1.62 ± 0.20; *n* = 15); the two outliers had strong push-pull but only a single prominent response area.

We then compared the pattern of push and pull for simple cells to that for thalamic relay cells (**Fig. 4b,c**), which are widely held to have segregated On and Off subregions (**Fig. 1a**). The values for the push-pull index, measured from the center subregion of the thalamic field, were 0.00–0.59 (0.10 ± 0.14; *n* = 25; **Fig. 4b)**. To estimate the relative spatial distribution of push and pull for simple and relay cells, we expanded the use of the overlap index (**Fig. 4c**). For each subregion, we compared the area of push response (excitation evoked by stimuli of the preferred contrast, fitted with an elliptical Gaussian) with the corresponding pull response (inhibition evoked by stimuli of the opposite contrast, fitted with an elliptical Gaussian). The results show that the push and pull largely overlap; values ranged from 0.30–0.91 (0.59 ± 0.17; *n* = 26) for simple cells and 0.17–0.96 (0.72 ± 0.19; *n* = 25) for relay cells. Note that these values may underestimate the actual overlap because weak inhibition was sometimes difficult to visualize. Overall, the scores for simple and relay cells were similar but not identical; the slight disparity might reflect mild asymmetries in the arrangement of excitation and inhibition in the two types of receptive fields.

Laminar distribution of receptive fields

How do these different receptive field profiles correlate with position in the cortical microcircuit? We plotted the distribution of the overlap index (**Fig. 5a**), number of segregated On and Off subregions (**Fig. 5b**) and push-pull index (**Fig. 5c**) according to laminar location. The profiles show that values for each parameter vary with depth in the cortical column. Cells whose receptive fields had scores that indicated simpleness (small values of overlap and push-pull indices and multiple subregions) were located only in layer 4 and the upper half of layer 6, where the thalamic afferents terminate (see **Fig. 7**). By contrast, neurons whose scores indicated complexness were found in all layers, though response pattern varied with laminar location. For example, complex cells in thalamorecipient zones always responded to both bright and dark sparse-noise stimuli, so the push-pull and overlap indices were near the maximum values. Conversely, cells in positions farther removed from the thalamus (layers 2+3, layer 5 and lower layer 6) seldom responded to the sparse noise; when they did respond, the push-pull index values were ≈1 because responses were limited to stimuli of one polarity: either bright or dark.

The relationship between scores for the overlap and push-pull indices for cells in the different cortical layers is depicted in a scatter plot (**Fig. 6**; color-coded for laminar location). The resulting distribution forms two clouds that represent statistically significant groups. If simple receptive fields are defined as having separated On and Off subregions with push-pull, the plot shows that simple cells are confined to thalamorecipient zones. The remaining heterogeneous group of cells, which we call complex, is distributed through the cortical depth. Notably, layer 4 and bordering regions contain the cells with the greatest degree of separation between On and Off subregions (5 of 9 smooth cells and 17 of 25 spiny neurons, mostly spiny stellate cells from layer 4) as well as those with the highest degree of overlap[7,11] (4 of 9 smooth cells and 5 of 25 spiny neurons, 3 pyramids at the borders of layer 4 and 2 spiny stellate cells). The remaining neurons had receptive fields composed of a single region, 2 (in layer 4) with a push-pull profile and 1 (at the 4–5 border) with a push-null profile.

Last, we used Pearson's correlation coefficient to compare the raw responses to bright and dark stimuli point by point, as others[29,32] have done to measure the segregation of On and Off

subregions. The resulting distribution (not shown) was similar to that for the overlap index ($r = 0.94783$, $P < 0.0001$) as well as to that for the push-pull index ($r = 0.93202$, $P < 0.0001$).

A plot of the laminar position of cells with simple receptive fields (**Fig. 7**) gives the strong impression that simple cells in lower layer 4 have more compact subregions than those in the middle or upper parts of the layer, although our sample was not large enough to allow us to establish definitive sublaminar patterns. Also, multiple subregions were more common in the middle to upper half of layer 4. Last, receptive fields built of very long subregions were found in layers 4 and 6, as indicated in an earlier physiological study[39].

Morphology and receptive field structure

Finally, we found no systematic associations between receptive field structure and general anatomical class, except for stereotyped laminar variations in morphology[1,3,4,10] (see summary of reconstructions, **Fig. 8**). We found simple (**Fig. 8a**) and complex (**Fig. 8b**) spiny stellate cells and smooth cells in layer 4, simple pyramids at the borders of layer 4 or the upper half of layer 6, and complex pyramids and smooth cells throughout the cortical depth. On a more subtle level, our past work[40] has shown that simple pyramidal cells in layer 6 have different dendritic branching patterns and axonal termination zones from complex pyramidal cells in layer 6. Perhaps future studies will show similar trends for neurons in other layers.

DISCUSSION

Each layer of cortex is characterized by a unique profile of connections[1,3,4,10,40]. The goal of our study was to understand the structure of the receptive fields that these different circuits build. The approach we used, whole-cell recording with dye-filled electrodes, provided two key advantages over traditional extracellular recordings. First, it was possible to label the cells from which we recorded to ascertain their laminar location and, hence, their position in the microcircuit. Second, the method revealed the synaptic structure of responses by showing subthreshold excitation as well as inhibition. Two main indices, an overlap index[33] and a push-pull index, allowed us to quantify the spatial relationship between On and Off responses and the presence of excitation (push) and/or inhibition (pull) within each receptive field. Cells with simple receptive fields (adjacent On and Off subregions with push-pull) were restricted to the first stage of cortical processing. The receptive fields of the remaining neurons, namely the complex cells, were heterogeneous, although stereotyped patterns correlated with separate positions in the microcircuit. Thus, different neural circuits play distinct roles in cortical processing.

Receptive field structure at the first cortical stage

By combining morphological identification with quantitative mapping of the receptive field, our experiments show that simple cells are confined to regions that receive direct thalamic input: layer 4, its borders and upper layer 6. Simple receptive fields have scores for the overlap index ($<<0.1$) indicating segregated On and Off subregions. Additionally, the scores for the push-pull index ($<<1$) show that stimuli of the reverse contrast evoke responses of the opposite sign. Thus, a clear view of the simple receptive field emerges when the spatial distribution of excitation and inhibition are taken into account. Furthermore, we have found that the values of the push-pull index measured from simple cells are similar to those measured from the centers of thalamic relay cells, indicating that this arrangement is carried forth from geniculate to cortex. Our current study, which places simple cells in thalamorecipient zones, is consistent with the idea that simple receptive fields are built by the convergence of thalamic inputs[12,23,26,41]. Thus, our results can be understood in the context of feed-forward models of orientation selectivity[26,37,42].

Layer 4 and its borders also contain a second, smaller population of cells (24% of the spiny neurons and 44% of the smooth cells) whose receptive fields have largely superimposed On and Off subfields (overlap index >0.35; push-pull index >1.34). Indeed, these cells have scores for the overlap and push-pull indices at the upper bounds of both distributions. Such 'first-order' complex cells may well correspond to types of nonsimple cells (complex and/or non-oriented concentric cells) that receive synaptic contacts from the lateral geniculate nucleus[7,43]. Although the layout of the receptive fields of these first-order complex cells is different from that of neighboring simple cells, both groups share a common synaptic physiology; as well the responses of all cells in layer 4 follow the time-course of thalamic drive[11].

A natural question is whether the first-order complex cells are orientation selective. Recent studies have shown that inhibitory complex cells in layer 4 were not tuned for stimulus orientation and have suggested that they might serve various roles in the global regulation of excitability[36,37,43]. As yet, it is unclear whether spiny complex cells in layer 4 are orientation selective and what their functional role might be.

Finally, we wonder whether the sublaminar differences in receptive field structure that we have observed relate to the anatomical organization of the primate's visual cortex. Specifically, we have found that simple cells with compact subfields are more common in the deeper aspect of layer 4, whereas those with narrower subregions are more frequent in the upper half of the layer. In the monkey, receptive fields in lower layer 4 are rounder than in the higher tiers, a difference that covaries with the distribution of parvocellular versus magnocellular inputs[13,44].

Receptive field structure at later cortical stages

The robust On and Off responses that sparse-noise stimuli routinely evoke in layer 4 are rare in layers 2+3, 5 and lower 6. At these later stages of cortical processing, most cells respond primarily to flashed stimuli of only one polarity (push-null) or do not respond to the static stimulus at all. Evoked responses are briefer and less reliable than in layer 4. Although cells in all layers respond vigorously to moving bars, these stimuli never evoked a push-pull pattern of response in layers 2+3, 5 or lower 6 (ref. 16). In general, responses at later stages of processing seem heterogeneous, unlike the situation in layer 4, where receptive fields divide into one of two clusters (**Fig. 6**). Similar differences in complex cell profile have been reported earlier, notably between the classes C2 and C1 (ref. 22). Here we extend this observation by demonstrating a correlation between response type and cortical location.

Laminar distribution of simple and complex cells

Our results support some earlier studies in the cat that have placed simple cells at the first stage of cortical processing and have found a broader distribution of various classes of complex cells[7,9,12]. Other studies have reported simple and complex cells throughout the cortical depth[15,32] (M.S. Jacob *et al., Soc. Neurosci. Abstr.* 910.13, 2003). We believe this discrepancy reflects variations in the nomenclature or criteria used for classification. First, there are different definitions of simple receptive fields, some of which include cells that are excited by only one polarity of the stimulus (S1). Thus, a cell classified as S1 by some investigators could be classified as complex by others, including ourselves. Indeed there are many terms for cells that respond to only one stimulus polarity, including complex[9,12], A[45], C1 or S1 (refs. 7,15, 22,45), discrete complex[38], Eon or Eoff[46] and monocontrast[13]. It seems likely, therefore, that the push-null responses that we have recorded from layers 2+3, 5 or 6 might have been called simple by others.

A second method of distinguishing simple from complex cells is based on response linearity rather than spatial structure of the receptive field. Earlier results have suggested that drifting sinusoidal gratings evoke linear responses from cells with separate On and Off subregions but nonlinear responses from cells with cospatial On and Off subfields[38,47]. Recent work in primates, however, has challenged the assumption that the spatial structure of the receptive field and linearity of response necessarily correlate[13]. Also, we think that the cells sensitive to only one stimulus contrast (such as push-null) would probably respond to gratings in a linear fashion. Hence, the observation that cells with linear responses are found throughout the cortical depth is not in apparent conflict with our results. Rather, it seems likely that there may be multiple ways to generate linear responses in the different cortical layers.

Are simple cells a distinct population?

There is current debate about whether simple and complex cells divide into two general classes or represent two ends of a continuous distribution[29,32,48]. Although the parameters we have measured are not unimodally distributed, we understand the potential for nonlinear output effects to change the shape of the distributions and current limitations of recording and spatial mapping techniques (see Methods). In any case, the strength of our result is that cells with low scores for both the overlap and the push-pull indices are found only in layer 4. Had we obtained unimodal distributions of both indices but found that all cells that fell below a certain cutoff were in layer 4, whereas all others were distributed in other cortical layers, our conclusions would be the same: that simple receptive fields represent an exclusive feature of the first stages of cortical processing. Thus, model circuits for simple cells in the cat should be constrained to components of the layers where thalamic afferents terminate.

Comparable studies of diverse species and sensory systems

Anatomical evidence emphasizes the importance of laminar specialization: the projection patterns of axons and dendrites grow more spatially precise with progression from rodent to carnivore to primate[1–3,15]. Our results contribute to the idea that connections in different layers are specialized for different tasks. Although we do not anticipate that receptive field structure *per se* will always vary with cortical layer, there is substantial evidence that different response properties arise at successive stages of cortical processing. The tree shrew's visual cortex provides a dramatic example. There, orientation tuning (absent in layer 4) emerges in the superficial layers, a development thought to arise from specific patterns of inter- and intralaminar convergence[17,49]. Likewise, in the monkey, orientation tuning and dynamics change as a function of laminar location[20]. Furthermore, we have previously shown that the relative orientation tuning of excitatory and inhibitory inputs varies substantially from the superficial to the deep layers in the cat[16].

Systematic changes in response properties are observed in other sensory modalities as well. For example, in rodent somatosensory cortex, receptive field structure, orientation selectivity and plasticity change from layer 4 to the superficial and deep layers[5,6,50]. In the auditory cortex, response properties such as inhibitory-side band structure (analogous to the antagonistic subregions of the simple receptive field) and bandwidth seem to vary with laminar location[14]. Our hope is that a better understanding of the structure and function of the visual cortical microcircuit will expose fundamental principles of neocortical processing.

METHODS

Physiological preparation. Anesthetized adult cats (1.5–3.5 kg) were prepared as described earlier[35]. All procedures were in accordance with the guidelines of the US National Institute of Health and the Institutional Animal Care and Use Committees of the Rockefeller University and the University of Southern California.

Recording, data acquisition and membrane properties. The methods for recordings were identical to those used in earlier studies[11,16,35,36,40]. Voltage-current relationships were measured before and after each stimulus cycle to monitor changes in access and input resistances, spike threshold and membrane time constant (6–28 ms, smooth cells; 11–32 ms, spiny cells). Recordings lasted from 0.3 to 5 h. It was often impractical to assign absolute resting potential, as the ratio of access to seal resistance led to a voltage division in the neural signal.

Receptive field mapping. Receptive fields were hand plotted to position the stimulus monitor and then mapped quantitatively with modified[35] sparse noise[21]; individual light and dark squares were flashed briefly (31–47 ms) in pseudorandom order, 16 times each on a 16 × 16 square grid; stimulus size was 0.85 or 1.7°, and contrast was 50 or 70%. Plots of receptive fields were made in two ways: as contour plots, where each concentric line represents a 10% reduction in response strength, or as arrays of trace pairs. For cells with spatially segregated On and Off subregions, contour plots were made by subtracting dark from bright responses. For overlapping On and Off subfields, plots for bright and dark stimuli, centered on the same spatial coordinates, are shown separately. For the arrays of trace pairs, each position on the stimulus grid is represented by two stacked traces showing the (spike-subtracted) average to all bright and dark stimuli flashed there.

Measuring synaptic excitation and inhibition. For responses evoked from each coordinate within the receptive field, excitation (net depolarization) was defined as the area of the synaptic response that was above rest (the averaged membrane potential in the prestimulus condition) within a fixed time interval centered near the peak response (~20–80 ms after stimulus presentation)[11,35,36]. Inhibition (net hyperpolarization) was defined as the area between rest and more negative voltages in the same time window. We sometimes made recordings at different membrane levels for the same cell. In those instances, the visually evoked hyperpolarization grew smaller at more negative membrane potentials, consistent with the idea that it was produced by inhibitory inputs rather than withdrawal of excitation[16,35].

Measuring receptive field structure. We combined different measures to analyze the spatial relationship between excitation and inhibition in the receptive fields. First, we gauged the spatial relationship of On and Off excitatory responses by means of an overlap index[33]:

$$\text{Overlap index} = \frac{0.5W_p + 0.5W_n - d}{0.5W_p + 0.5W_n + d} \quad (1)$$

where W_p and W_n are the widths of the On and Off subregions, respectively, and d is the distance between the peak positions of each subregion (measured from the synaptic response areas, as above). The value of the index is ≤0 for separated subregions and approaches 1 for subregions that overlap symmetrically.

The parameters for the overlap index, W_p, W_n and d, were determined by separately fitting each On and Off excitatory response region with an elliptical Gaussian:

$$f(x, y) = \frac{A}{2\pi ab}\exp\left(-\frac{x'^2}{2a^2} - \frac{y'^2}{2b^2}\right) \quad (2)$$

for which A determines the maximum amplitude, a and b are the half axes of the ellipse, and x' and y' are transformations of the stimulus coordinates x and y, taking into account the angle θ and the offset (x_c and y_c) of the ellipse. Thus, there were six free parameters in the fitting procedure: A, a, b, θ, x_c and y_c.

Any measure of subfield overlap is subject to nonlinearities that could bias results towards greater segregation (simpleness) or overlap (complexness). For instance, the method we used

is based on Gaussian fits of the subregions; thus, it can overestimate the degree of overlap if On and Off subfields have very different amplitudes. Additionally, it cannot account for the weak borders of the subregions, which fall below the cutoff of the fitted Gaussian. Nonetheless, we prefer the overlap index to alternative measures such as the correlation coefficient[32], which can exaggerate actual overlap because stimuli that straddle the borders between subregions will evoke On and Off responses simultaneously[35]. This problem is exacerbated by the voltage dependence of the amplitudes of synaptic potentials. Still, to relate our measures to others (e.g., ref. [32]), we evaluated our results with Pearson's correlation coefficient:

$$r = \frac{\sum_{i=1}^{n}\left(R_{on_i} - \bar{R}_{on}\right)\left(R_{off_i} - \bar{R}_{off}\right)}{\sqrt{\sum_{i=1}^{n}\left(R_{on_i} - \bar{R}_{on}\right)^2 \sum_{i=1}^{n}\left(R_{off_i} - \bar{R}_{off}\right)^2}} \quad (3)$$

where R_{on} is the response to all bright squares and R_{off} the response to all dark squares that fell within the receptive field.

Our second measure, the push-pull index, gauged the presence and relative magnitude of antagonistic responses to stimuli of the reverse contrast within each subfield:

$$\text{Push} - \text{pull index} = |P + N| \quad (4)$$

where P and N represent synaptic responses to bright and the dark stimuli, respectively. The value of the index was ≈0 when stimuli of the opposite contrast evoked excitatory and inhibitory responses of comparable magnitude (**Fig. 4a**, bottom). Values ≈1 indicated that stimuli of only one contrast generated significant responses[11] and scores ≈2 indicated that bright and dark stimuli evoked responses of the same sign and similar strength. We confined our measurement to the center of each subregion because our stimuli were often large and sometimes seemed to overlap subregions[35]. We normalized the measures for push and pull because the relative strength of each depends strongly on membrane potential[35]. Although we recorded at membrane levels set to show both excitation and inhibition, it was impossible to achieve equivalent recording conditions in every cell. Notably, however, we calculated the index without normalizing and found little change in the shape of the distribution of values (not shown).

Last, we expanded the use of the overlap index to estimate the relative spatial distribution of push and pull within individual subfields (that is, to compare excitatory and inhibitory responses evoked by bright and dark spots flashed in the same subregion). If the push and pull were largely cospatial, the values of the index approached 1.

Histology. After histological processing[35], labeled neurons were drawn using a computerized three-dimensional reconstruction system (Microbrightfield).

ACKNOWLEDGMENTS

We thank T.N. Wiesel for support over the years and C.G. Marshall, K.D. Naik and J.M. Provost for assistance with the anatomical reconstructions. Supported by US National Institutes of Health grant EY09593 to J.A.H.

COMPETING INTERESTS STATEMENT

The authors declare that they have no competing financial interests.

References

1. Callaway EM. Local circuits in primary visual cortex of the macaque monkey. Annu. Rev. Neurosci 1998;21:47–74. [PubMed: 9530491]

2. Fitzpatrick D. The functional organization of local circuits in visual cortex: insights from the study of tree shrew striate cortex. Cereb. Cortex 1996;6:329–341. [PubMed: 8670661]
3. Lund JS, Henry GH, MacQueen CL, Harvey AR. Anatomical organization of the primary visual cortex (area 17) of the cat. A comparison with area 17 of the macaque monkey. J. Comp. Neurol 1979;184:599–618. [PubMed: 106072]
4. Binzegger T, Douglas RJ, Martin KA. A quantitative map of the circuit of cat primary visual cortex. J. Neurosci 2004;24:8441–8453. [PubMed: 15456817]
5. Brecht M, Roth A, Sakmann B. Dynamic receptive fields of reconstructed pyramidal cells in layers 3 and 2 of rat somatosensory barrel cortex. J. Physiol. (Lond.) 2003;553:243–265. [PubMed: 12949232]
6. Brumberg JC, Pinto DJ, Simons DJ. Cortical columnar processing in the rat whisker-to-barrel system. J. Neurophysiol 1999;82:1808–1817. [PubMed: 10515970]
7. Bullier J, Henry GH. Ordinal position of neurons in cat striate cortex. J. Neurophysiol 1979;42:1251–1263. [PubMed: 226663]
8. Contreras D, Palmer LA. Response to contrast of electrophysiologically defined cell classes in primary visual cortex. J. Neurosci 2003;23:6936–6945. [PubMed: 12890788]
9. Gilbert CD. Laminar differences in receptive field properties of cells in cat primary visual cortex. J. Physiol. (Lond.) 1977;268:391–421. [PubMed: 874916]
10. Gilbert CD, Wiesel TN. Morphology and intracortical projections of functionally characterised neurones in the cat visual cortex. Nature 1979;280:120–125. [PubMed: 552600]
11. Hirsch JA, et al. Synaptic physiology of the flow of information in the cat's visual cortex in vivo. J. Physiol. (Lond.) 2002;540:335–350. [PubMed: 11927691]
12. Hubel DH, Wiesel TN. Receptive fields, binocular interaction and functional architecture in the cat's visual cortex. J. Physiol. (Lond.) 1962;160:106–154. [PubMed: 14449617]
13. Kagan I, Gur M, Snodderly DM. Spatial organization of receptive fields of V1 neurons of alert monkeys: comparison with responses to gratings. J. Neurophysiol 2002;88:2557–2574. [PubMed: 12424294]
14. Linden JF, Schreiner CE. Columnar transformations in auditory cortex? A comparison to visual and somatosensory cortices. Cereb. Cortex 2003;13:83–89. [PubMed: 12466219]
15. Martin KA, Whitteridge D. Form, function and intracortical projections of spiny neurons in the striate visual cortex of the cat. J. Physiol. (Lond.) 1984;353:463–504. [PubMed: 6481629]
16. Martinez LM, Alonso JM, Reid RC, Hirsch JA. Laminar processing of stimulus orientation in cat visual cortex. J. Physiol 2002;540:321–333. [PubMed: 11927690]
17. Mooser F, Bosking WH, Fitzpatrick D. A morphological basis for orientation tuning in primary visual cortex. Nat. Neurosci 2004;8:872–879. [PubMed: 15258585]
18. Nowak LG, Azouz R, Sanchez-Vives MV, Gray CM, McCormick DA. Electrophysiological classes of cat primary visual cortical neurons in vivo as revealed by quantitative analyses. J. Neurophysiol 2003;89:1541–1566. [PubMed: 12626627]
19. Swadlow HA, Hicks TP. Somatosensory cortical efferent neurons of the awake rabbit: latencies to activation via supra- and subthreshold receptive fields. J. Neurophysiol 1996;75:1753–1759. [PubMed: 8727411]
20. Ringach DL, Shapley R, Hawken MJ. Orientation selectivity in macaque V1: diversity and laminar dependence. J. Neurosci 2002;22:5639–5651. [PubMed: 12097515]
21. Jones JP, Palmer LA. The two-dimensional spatial structure of simple receptive fields in cat striate cortex. J. Neurophysiol 1987;58:1187–1211. [PubMed: 3437330]
22. Palmer LA, Davis TL. Receptive-field structure in cat striate cortex. J. Neurophysiol 1981;46:260–276. [PubMed: 6267213]
23. Ferster D. Spatially opponent excitation and inhibition in simple cells of the cat visual cortex. J. Neurosci 1988;8:1172–1180. [PubMed: 3357015]
24. Chapman B, Zahs KR, Stryker MP. Relation of cortical cell orientation selectivity to alignment of receptive fields of the geniculocortical afferents that arborize within a single orientation column in ferret visual cortex. J. Neurosci 1991;11:1347–1358. [PubMed: 2027051]
25. Reid RC, Alonso JM. Specificity of monosynaptic connections from thalamus to visual cortex. Nature 1995;378:281–284. [PubMed: 7477347]

26. Ferster D, Miller KD. Neural mechanisms of orientation selectivity in the visual cortex. Annu. Rev. Neurosci 2000;23:441–471. [PubMed: 10845071]
27. Chance FS, Nelson SB, Abbott LF. Complex cells as cortically amplified simple cells. Nat. Neurosci 1999;2:277–282. [PubMed: 10195222]
28. Borg-Graham LJ, Monier C, Fregnac Y. Visual input evokes transient and strong shunting inhibition in visual cortical neurons. Nature 1998;393:369–373. [PubMed: 9620800]
29. MataMLRingachDLSpatial overlap of On and Off subregions and its relation to response modulation ratio in macaque primary visual cortex. J. Neurophysiol(in the press)
30. Rivadulla C, Sharma J, Sur M. Specific roles of NMDA and AMPA receptors in direction-selective and spatial phase-selective responses in visual cortex. J. Neurosci 2001;21:1710–1719. [PubMed: 11222660]
31. Tao L, Shelley M, McLaughlin D, Shapley R. An egalitarian network model for the emergence of simple and complex cells in visual cortex. Proc. Natl. Acad. Sci. USA 2004;101:366–371. [PubMed: 14695891]
32. Priebe NJ, Mechler F, Carandini M, Ferster D. The contribution of spike threshold to the dichotomy of cortical simple and complex cells. Nat. Neurosci 2004;7:1113–1122. [PubMed: 15338009]
33. Schiller PH, Finlay BL, Volman SF. Quantitative studies of single-cell properties in monkey striate cortex. I. Spatiotemporal organization of receptive fields. J. Neurophysiol 1976;39:1288–1319. [PubMed: 825621]
34. De Angelis GC, Ohzawa I, Freeman RD. Receptive field dynamics in central visual pathways. Trends Neurosci 1995;18:451–458. [PubMed: 8545912]
35. Hirsch JA, Alonso JM, Reid RC, Martinez LM. Synaptic integration in striate cortical simple cells. J. Neurosci 1998;18:9517–9528. [PubMed: 9801388]
36. Hirsch JA, et al. Functionally distinct inhibitory neurons at the first stage of visual cortical processing. Nat. Neurosci 2003;6:1300–1308. [PubMed: 14625553]
37. Lauritzen TZ, Miller KD. Different roles for simple- and complex-cell inhibition in V1. J. Neurosci 2003;23:10201–10213. [PubMed: 14614078]
38. Dean AF, Tolhurst DJ. On the distinctness of simple and complex cells in the visual cortex of the cat. J. Physiol. (Lond.) 1983;344:305–325. [PubMed: 6655583]
39. Grieve KL, Sillito AM. A re-appraisal of the role of layer VI of the visual cortex in the generation of cortical end inhibition. Exp. Brain Res 1991;87:521–529. [PubMed: 1783022]
40. Hirsch JA, Gallagher CA, Alonso JM, Martinez LM. Ascending projections of simple and complex cells in layer 6 of the cat striate cortex. J. Neurosci 1998;18:8086–8094. [PubMed: 9742175]
41. Movshon JA, Thompson ID, Tolhurst DJ. Spatial summation in the receptive fields of simple cells in the cat's striate cortex. J. Physiol. (Lond.) 1978a;283:53–77. [PubMed: 722589]
42. Troyer TW, Krukowski AE, Priebe NJ, Miller KD. Contrast-invariant orientation tuning in cat visual cortex: thalamocortical input tuning and correlation-based intracortical connectivity. J. Neurosci 1998;18:5908–5927. [PubMed: 9671678]
43. Usrey WM, Sceniak MP, Chapman B. Receptive fields and response properties of neurons in layer 4 of ferret visual cortex. J. Neurophysiol 2003;89:1003–1015. [PubMed: 12574476]
44. Bullier J, Henry GH. Ordinal position and afferent input of neurons in monkey striate cortex. J. Comp. Neurol 1980;193:913–935. [PubMed: 6253535]
45. Henry GH. Receptive field classes of cells in the striate cortex of the cat. Brain Res 1977;133:1–28. [PubMed: 902079]
46. Toyama K, Kimura M, Tanaka K. Organization of cat visual cortex as investigated by cross-correlation analysis. J. Neurophysiol 1981;46:202–214. [PubMed: 6267212]
47. Skottun BC, et al. Classifying simple and complex cells on the basis of response modulation. Vision Res 1991;31:1079–1086. [PubMed: 1909826]
48. Mechler F, Ringach DL. On the classification of simple and complex cells. Vision Res 2002;42:1017–1033. [PubMed: 11934453]
49. Chisum HJ, Mooser F, Fitzpatrick D. Emergent properties of layer 2/3 neurons reflect the collinear arrangement of horizontal connections in tree shrew visual cortex. J. Neurosci 2003;23:2947–2960. [PubMed: 12684482]

50. Diamond ME, Huang W, Ebner FF. Laminar comparison of somatosensory cortical plasticity. Science 1994;265:1885–1888. [PubMed: 8091215]

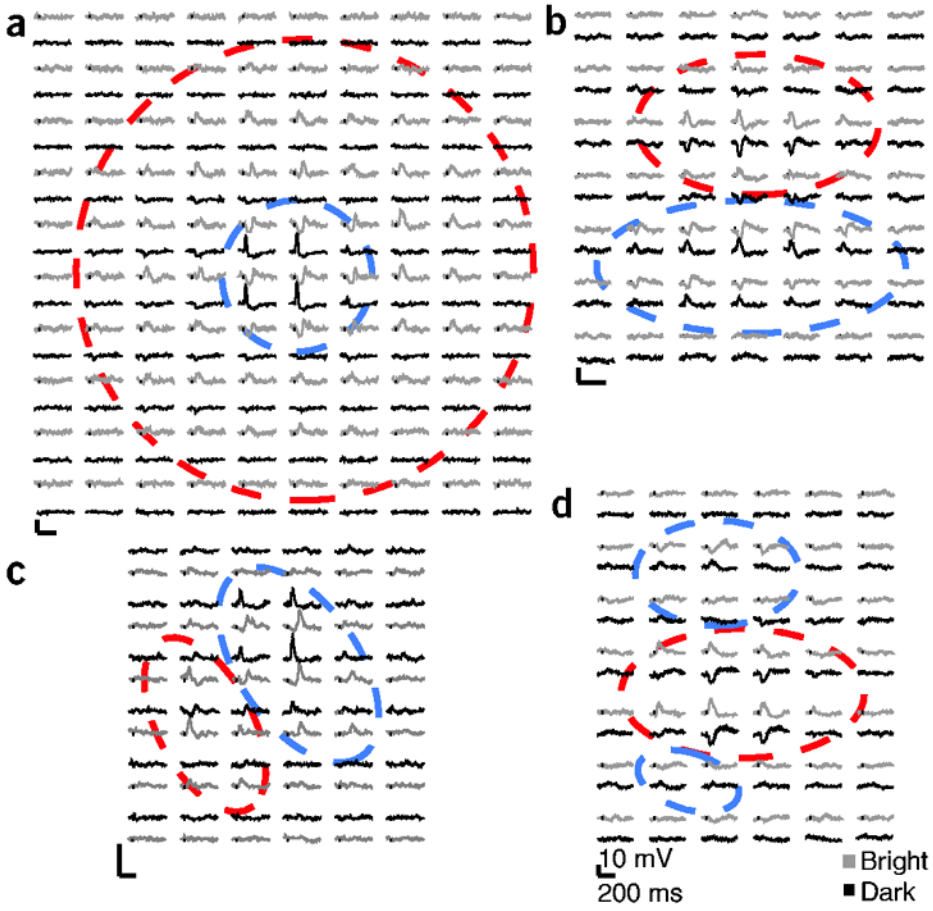

Figure 1.

Receptive fields with a push-pull arrangement of synaptic inputs. (**a**–**d**) Receptive fields of a thalamocortical neuron in the lateral geniculate nucleus (**a**), two spiny cells (**b**,**d**) and a smooth cell (**c**), all in layer 4. The receptive fields are shown as arrays of trace pairs in which each position in the stimulus grid is represented by averages of the corresponding responses to dark (black traces) and bright (gray traces) squares. The boundaries of On (red) and Off (blue) subregions are approximated by dashed circles or ovals. In all panels, stimuli of the reverse contrast evoked responses of the opposite sign (push-pull) in each subregion. The small vertical dashes indicate the onset of the stimulus, which was flashed for 31 or 47 ms; stimulus size was 0.85° or 1.7° and grid spacing was 0.85° (that is, each square in the array represents 0.85° of visual angle).

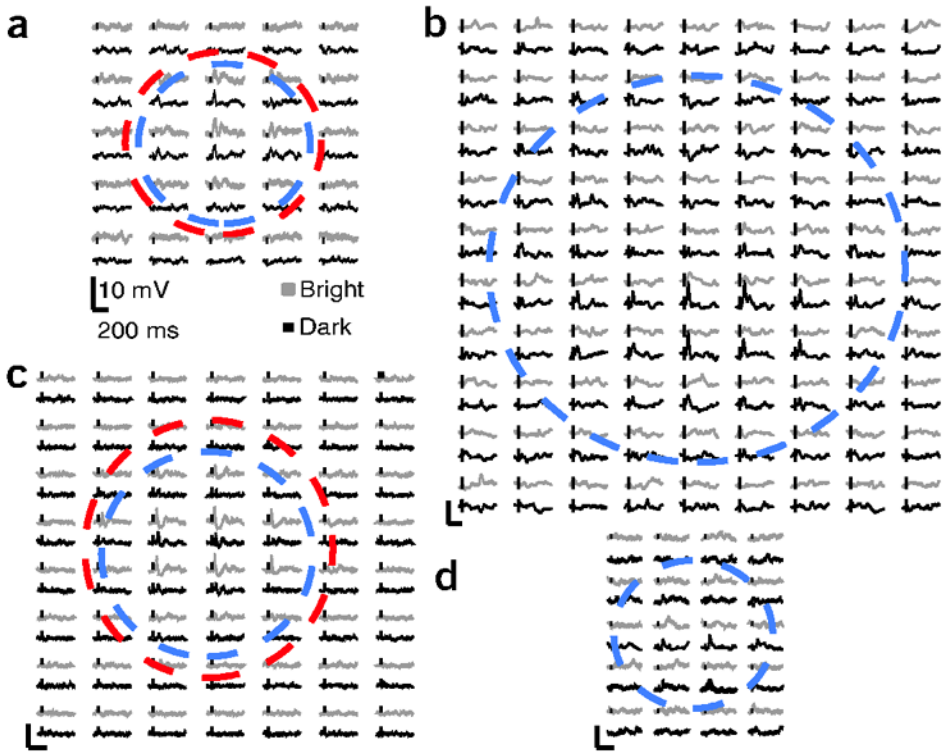

Figure 2.

Receptive fields with push-push or push-null configurations. (**a**–**c**) Receptive fields of a spiny stellate cell (**a**) and a smooth cell (**c**) in layer 4, a pyramidal cell in layers 2+3 (**b**) and a pyramidal cell in lower layer 6 (**d**); conventions as for **Figure 1**. Excitation to bright and dark stimuli was spatially overlapping (push-push) in the receptive fields from layer 4 (**a**,**c**). Outside layer 4, cells rarely responded to both polarities of the stimulus, so receptive fields often had just one subregion (push-null) (**b**,**d**) or could not be mapped with the sparse noise (not shown). Stimulus size was 0.85° or 1.7° and grid spacing was 0.85°.

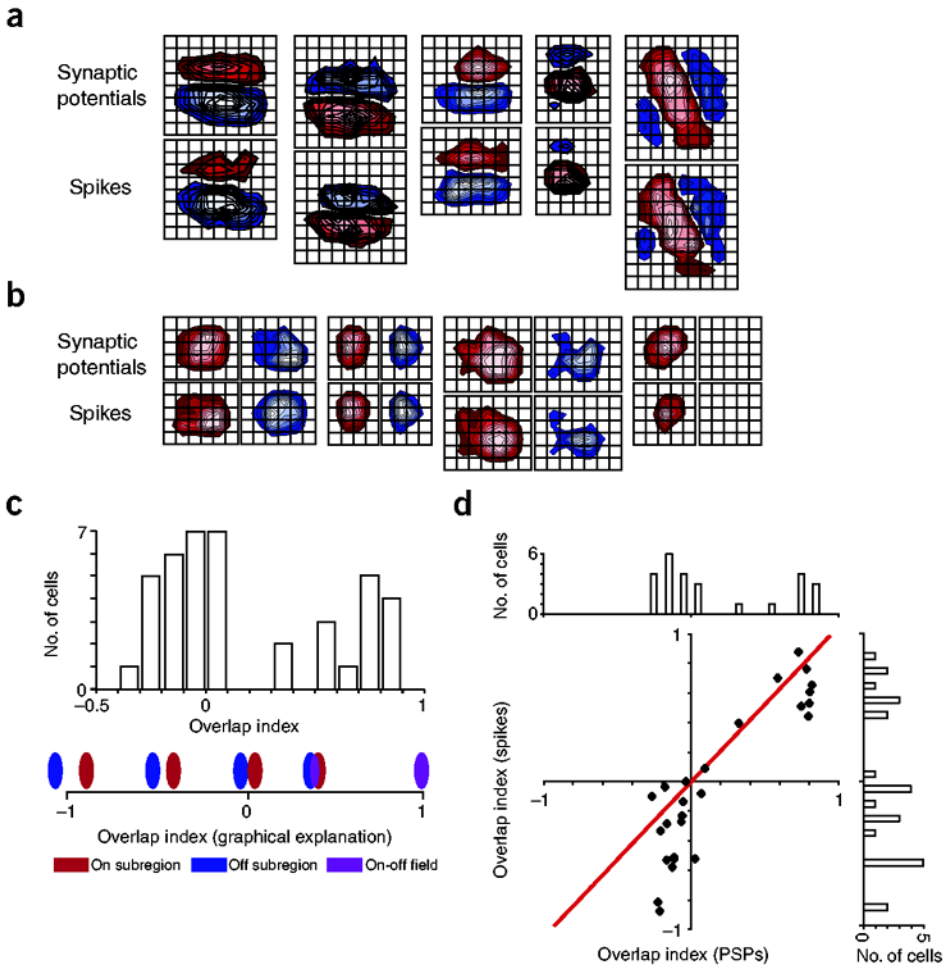

Figure 3.

The spatial arrangement of On and Off subregions in cortical receptive fields. (**a**,**b**) Contour plots of the receptive fields of five simple (**a**) and four complex cells (**b**) compare maps constructed from synaptic potentials to those made from spikes. For simple cells, On (red) and Off (blue) responses are shown in the same plot, and for complex cells, maps of On and Off responses are shown in separate panels. Each contour was smoothed and represents a 10% decrement relative to the peak (brightest) value; the maps were thresholded by 10%. The responses constructed from spikes were normalized separately from those made from synaptic potentials. Stimulus size was 0.85° or 1.7° and grid spacing was 0.85° (that is, the space between each line on the overlay is 0.85°). Overlap index values for simple cells from left to right were (synaptic potentials and spikes, respectively) −0.20, −0.34; 0.07, −0.08; −0.16, −0.29; −0.22, −0.82; −0.18, −0.04. For complex cells, they were 0.80, 0.53; 0.79, 0.76; 0.82, 0.66; 1 polarity, 1 polarity. (**c**) Histogram showing the distribution of values of overlap index (bin size = 0.1) for the entire population with a graphical explanation of the index below. Only cells that responded to both polarities of the stimulus were included. The distribution of values was not unimodal (probability of rejection 0.99, Hartigan's dip test). (**d**) The histograms at top and right show index values for synaptic excitation (as in **a**) and spikes (as in **b**), respectively. The central scatter plot compares the two sets of values for each cell; the red line indicates unit slope.

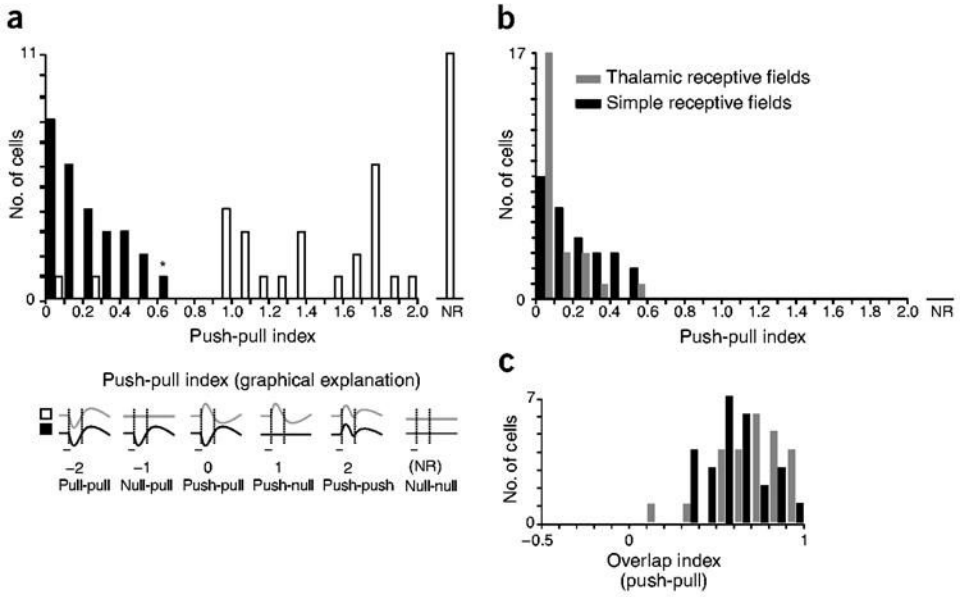

Figure 4.

Excitation and inhibition within single subregions of the receptive field. (**a**) Histogram of absolute values of the push-pull index (bin size = 0.1) with a graphical explanation of the index below. Filled bars, cells with segregated On and Off subregions (overlap index ≤0.09); open bars, cells with overlapping On and Off subfields (overlap index >0.3) or with just one subregion; NR indicates that there was no response to the flash stimulus. The asterisk marks a pyramid in layer 2+3 whose dendrites extended into layer 4 and whose receptive field had push-pull in only one of two subregions. The distribution of values was not unimodal, probability of rejection 0.99 (Hartigan's dip test). (**b**) Comparison of values of push-pull index for thalamic receptive fields (gray) and simple cortical receptive fields with segregated On and Off subregions (black); bin size = 0.1. (**c**) Overlap index values of excitatory and inhibitory responses to stimuli of the opposite contrast in thalamic receptive field centers (gray) and in the individual subfields of cortical cells with separated subregions (black); bin size = 0.1.

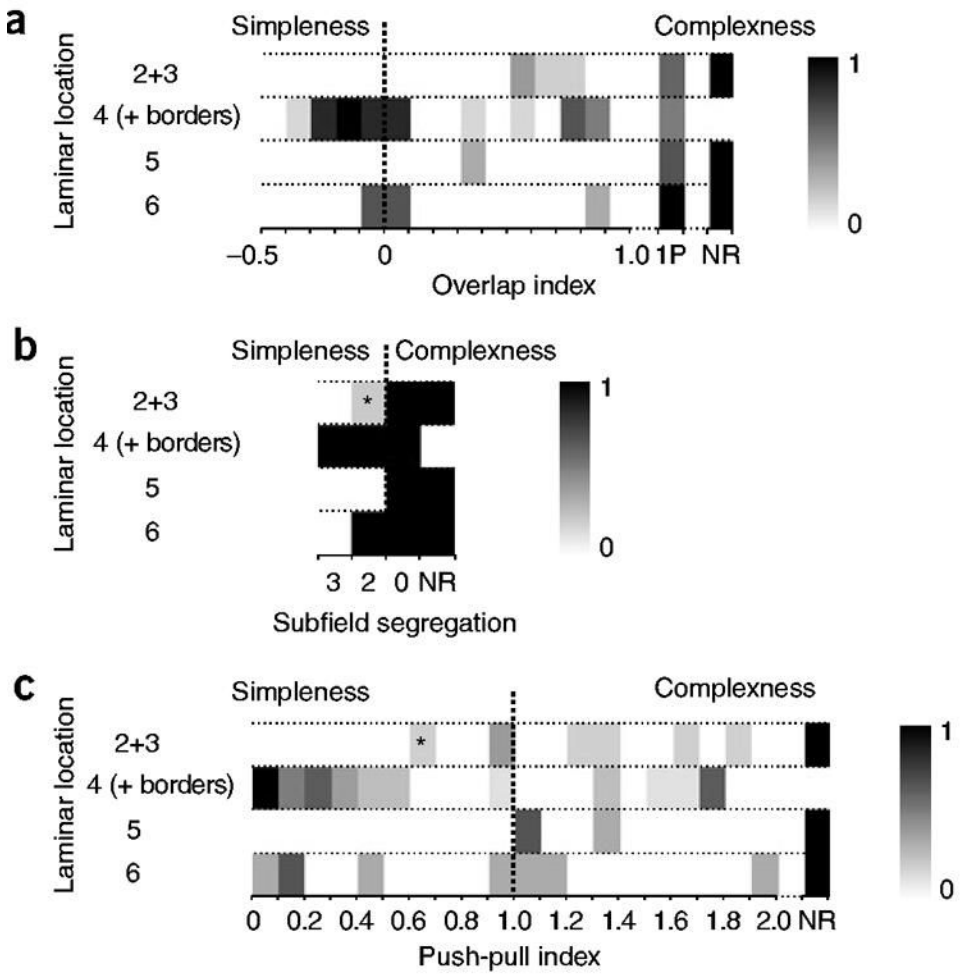

Figure 5.

Correlation between receptive field structure and cortical layer. (**a**–**c**) Histograms show the distribution of values for the overlap index (**a**), number of subregions (**b**) and push-pull index (**c**) in the different cortical layers. 1P indicates cells that responded to only one polarity of the sparse noise, and NR denotes cells that did not respond to the static stimulus at all; bin size was 0.1 in **a** and **c**. In each histogram, for each layer, the bin with the greatest number of cells is shaded black, and the gray level in the remaining bins is normalized to that maximum. For **b**, the bins are labeled by the number (2 or 3) of separated On and Off subregions; 0 includes cells with overlapped On and Off subregions and those that responded to only one stimulus polarity; asterisk same as for **Figure 4**.

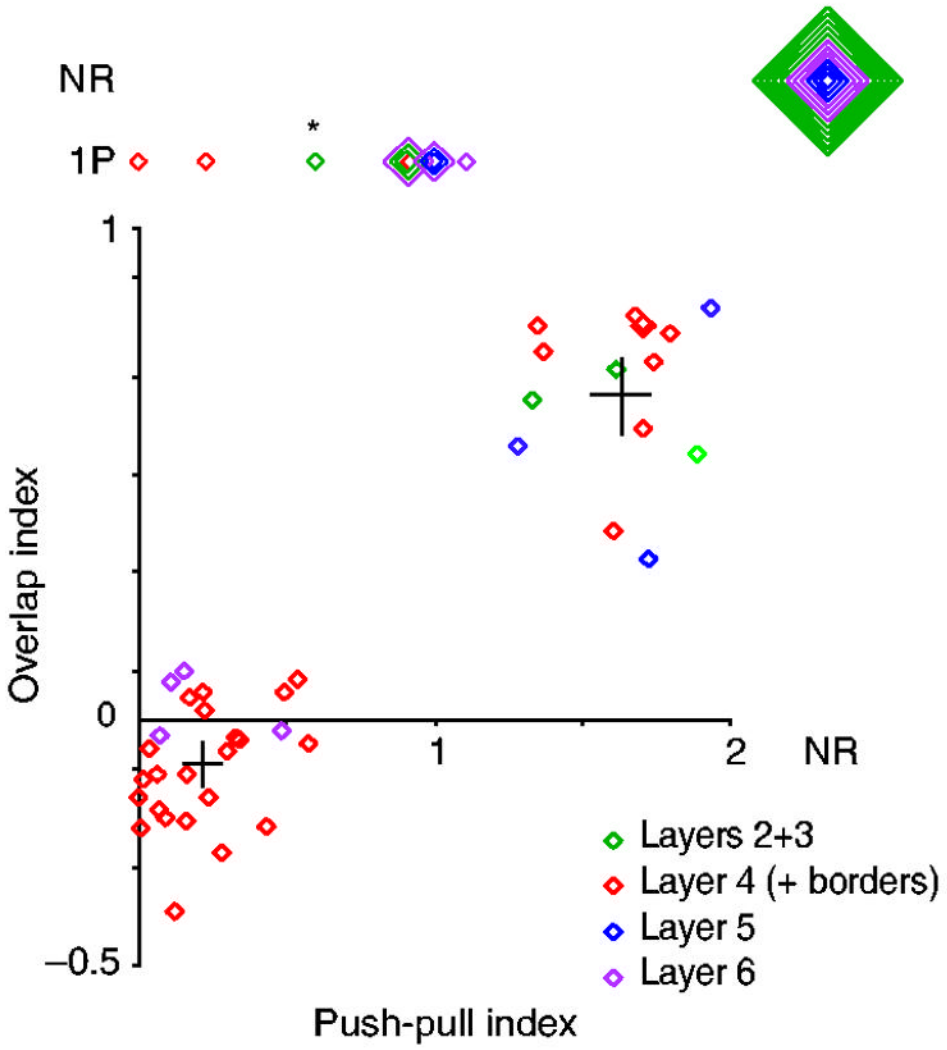

Figure 6.

Comparison of subregion overlap and push-pull. A scatter plot of subregion overlap versus push-pull; the results are color coded for layer. The points above the plot show push-pull index values for cells that responded to only one polarity of the stimulus (1P); the label NR indicates cells (upper right) that did not respond to the sparse noise. The intersection of the crosses in each cluster of points corresponds to the mean, and the length of each line to the 95% confidence intervals (calculated with a bootstrap method). Concentric symbols are used when multiple cells shared the same coordinate; asterisk as for **Figure 4**.

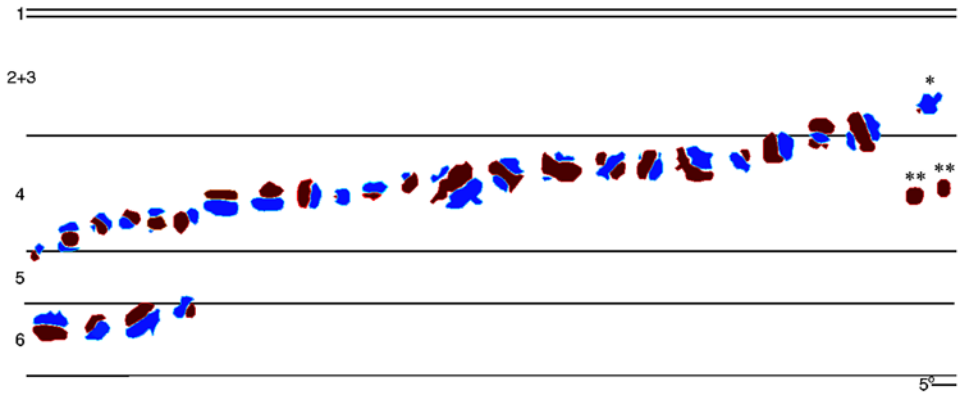

Figure 7.

Laminar distribution of receptive fields with push-pull. Receptive fields with a push-pull organization were found in layer 4, its borders or in upper layer 6, with one exception: a pyramid in layer 2+3 with dendrites extending into layer 4. The receptive fields are ordered from left to right according to depth of the soma. All but three of the receptive fields with push-pull had ≥2 subregions; On and Off subregions are red and blue, respectively, and asterisks indicate cells with only one obvious subregion. The scale bar (5°) indicates the size of the receptive fields.

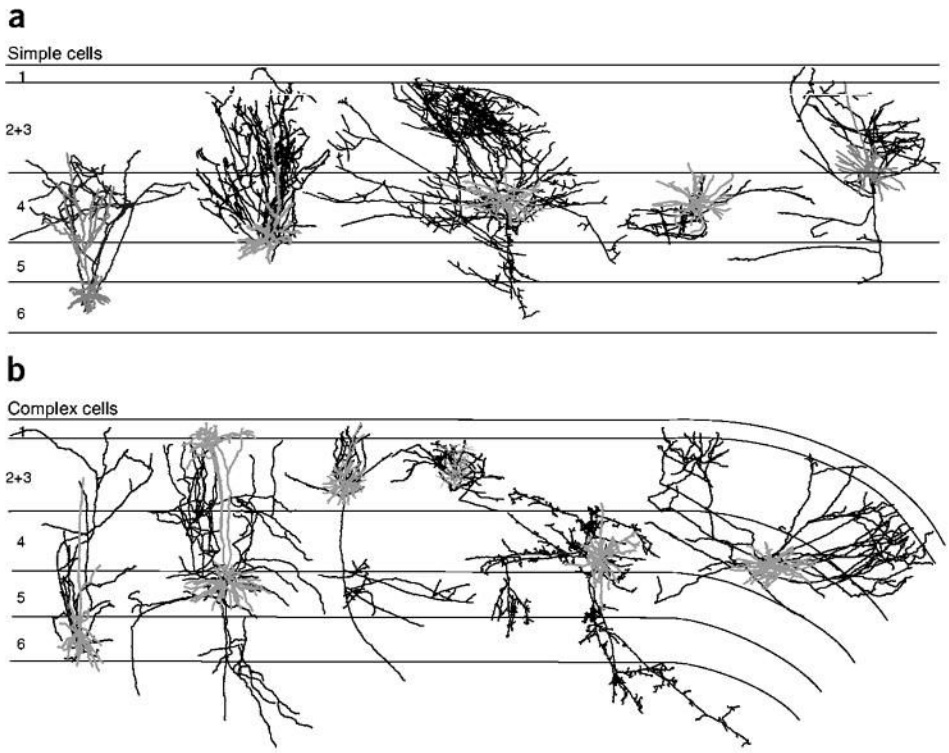

Figure 8.

Morphology and receptive field structure. (**a**,**b**) The figure shows a sample of our three-dimensional reconstructions taken from the simple cell (**a**) and complex cell (**b**) populations. The figure shows coronal views (from left to right, top) of a pyramid in upper layer 6, a pyramid at the 4–5 border, a spiny stellate cell in layer 4, a smooth cell in layer 4 and a pyramid at the 3–4 border; and (from left to right, bottom) of a pyramid in mid layer 6, a pyramid in layer 5, two pyramids in the superficial layers; a basket cell in layer 4 and a spiny stellate cell in the same layer. Cell bodies and dendritic arbors are gray, and axons are black.